REPORT DOCUMENTATION PAGE

Form Approved OMB NO. 0704-0188

1. REPORT DATE (DD-MM-YYYY)	2. REPORT TYPE	3. DATES COVERED (From - To)
	New Reprint	-

4. TITLE AND SUBTITLE
A QMUapproachforcharacterizingtheoperabilitylimitsofair-breathinghypersonic vehicles

5a. CONTRACT NUMBER	W911NF-09-1-0306
5b. GRANT NUMBER	
5c. PROGRAM ELEMENT NUMBER	611102
5d. PROJECT NUMBER	
5e. TASK NUMBER	
5f. WORK UNIT NUMBER	

6. AUTHORS
H.K. Lim, Y. Zhou, V.F. de Almeida, J. Glimm

7. PERFORMING ORGANIZATION NAMES AND ADDRESSES
Research Foundation of SUNY at Stony Brc
Office of Sponsored Programs
W-5510 Melville Library
Stony Brook, NY 11794 -3362

8. PERFORMING ORGANIZATION REPORT NUMBER

9. SPONSORING/MONITORING AGENCY NAME(S) AND ADDRESS (ES)
U.S. Army Research Office
P.O. Box 12211
Research Triangle Park, NC 27709-2211

10. SPONSOR/MONITOR'S ACRONYM(S)
ARO

11. SPONSOR/MONITOR'S REPORT NUMBER(S)
54161-MA.31

12. DISTRIBUTION AVAILIBILITY STATEMENT
Approved for public release; distribution is unlimited.

13. SUPPLEMENTARY NOTES
The views, opinions and/or findings contained in this report are those of the author(s) and should not contrued as an official Department of the Army position, policy or decision, unless so designated by other documentation.

14. ABSTRACT
The operability limits of a supersonic combustion engine for an air-breathing hypersonic vehicle are characterized using numerical simulations and an uncertainty quantification methodology. The time-dependent compressible flow equations with heat release are solved in a simplified configuration. Verification, calibration and validation are carried out to assess the ability of the model to reproduce the flow/thermal interactions that occur when the engine unstarts due to thermal choking. quantification of margins and uncertainty (QMU) isused to determine the safe operation region for a range of fuel

15. SUBJECT TERMS
QMU, Hypersonics, Scramjet, Intervals

16. SECURITY CLASSIFICATION OF:			17. LIMITATION OF ABSTRACT	15. NUMBER OF PAGES	19a. NAME OF RESPONSIBLE PERSON
a. REPORT	b. ABSTRACT	c. THIS PAGE			James Glimm
UU	UU	UU	UU		19b. TELEPHONE NUMBER 631-632-8370

Report Title

A QMUapproachforcharacterizingtheoperabilitylimitsofair-breathinghypersonic vehicles

ABSTRACT

The operability limits of a supersonic combustion engine for an air-breathing hypersonic vehicle are characterized using numerical simulations and an uncertainty quantification methodology. The time-dependent compressible flow equations with heat release are solved in a simplified configuration. Verification, calibration and validation are carried out to assess the ability of the model to reproduce the flow/thermal interactions that occur when the engine unstarts due to thermal choking. quantification of margins and uncertainty (QMU) isused to determine the safe operation region for a range of fuel flow rates and combustor geometries.

REPORT DOCUMENTATION PAGE (SF298)
(Continuation Sheet)

Continuation for Block 13

ARO Report Number 54161.31-MA
A QMUapproachforcharacterizingtheoperabilityli...

Block 13: Supplementary Note

Approved for public release; distribution is unlimited.

Reliability Engineering and System Safety 96 (2011) 1150–1160

Contents lists available at ScienceDirect

Reliability Engineering and System Safety

journal homepage: www.elsevier.com/locate/ress

A QMU approach for characterizing the operability limits of air-breathing hypersonic vehicles

Gianluca Iaccarino [a,*], Rene Pecnik [a], James Glimm [b], David Sharp [c]

[a] Mechanical Engineering Department, Stanford University, Stanford, CA 94305-3035, USA
[b] Applied Mathematics and Statistics Department, SUNY Stony Brook, NY 11794-3600, USA
[c] Los Alamos National Laboratory, Los Alamos, NM 87544, USA

ARTICLE INFO

Article history:
Received 20 February 2010
Received in revised form
11 June 2010
Accepted 15 June 2010
Available online 14 April 2011

Keywords:
QMU
Hypersonics
Scramjet
Intervals

ABSTRACT

The operability limits of a supersonic combustion engine for an air-breathing hypersonic vehicle are characterized using numerical simulations and an uncertainty quantification methodology. The time-dependent compressible flow equations with heat release are solved in a simplified configuration. Verification, calibration and validation are carried out to assess the ability of the model to reproduce the flow/thermal interactions that occur when the engine unstarts due to thermal choking. quantification of margins and uncertainty (QMU) is used to determine the safe operation region for a range of fuel flow rates and combustor geometries.

1. Introduction

Safety margins protect engineering devices against extreme load events, unexpected operating conditions, and manufacturing imperfections. Early design rarely takes into account reliability and, as a result, safety factors are applied as *a posteriori* corrections; these are typically based on experience and change radically in different application areas.

There is a general lack of well-defined procedures to objectively quantify the confidence in the *operability* of an engineering system. Complex devices, such as aerospace systems, are typically difficult to characterize in a satisfactory way. The behavior of a complex engineering device is also typically characterized by a large number of parameters; failures typically occur in response to one of the operating conditions exceeding a permissible threshold, e.g. exceeding structural load. In addition, unexpected (hidden) correlations between physical processes can lead to failure in response to a sequence of events with each parameter remaining within the allowable range of operation.

The *operation region* is the environment in which the device of interest is designed and expected to operate successfully; mathematically we define this region as the admissible volume Ω_{or} in the space of all the parameters affecting the behavior of the system. Γ_{or} is the boundary of such a region and is defined as the locus of the *unsafe* operating conditions; these do not necessarily represent failure points, but cases for which no positive evidence of acceptable performance exists; we refer to them more precisely as the *performance thresholds*.

The intuitive notion of safe operation of the device implies a *distance* (margin) from the performance threshold and therefore a parameter space Ω_s smaller than the operating region ($\Omega_s \subset \Omega_{or}$, see Fig. 1). The main difficulty in determining the margin is the presence of uncertainties in both the precise location of the cliffs (Γ_{or}) and the actual operating conditions of the system (the location in Ω_{or}). These uncertainties are due to variability in the environment the system is operating in, manufacturing tolerances, material imperfections (*aleatory* uncertainties), and to our limited understanding of the physical processes at play (*epistemic* uncertainties). As a result, a purely deterministic evaluation of the margin is not sufficient and probabilistic approaches, or more generally, approaches that directly account for the uncertainties have to be considered.

Quantification of Margin and Uncertainties (QMU) is a methodology created to facilitate analysis and communication of confidence for certification of complex systems [1]. In QMU the confidence is defined in a deceptively simple way:

$$CR = \frac{M}{U}$$

where M is the a measure of the *margin* and U a measure of the uncertainty. CR is the confidence ratio which has to be evaluated for the full system (and for the subsystems) in the operating

* Corresponding author.
E-mail address: giaccarino@gmail.com (G. Iaccarino).

0951-8320/$ - see front matter © 2011 Elsevier Ltd. All rights reserved.
doi:10.1016/j.ress.2010.06.030

region Ω_s of the device. A *CR* sufficiently larger than one intuitively indicates safe conditions.

The theoretical framework for QMU and the open questions related to its applicability are discussed in a number of articles and reports, for example [2–6]. Detailed applications of QMU to real-world engineering studies are limited because of the difficulties in assessing the predictive capabilities of complex computational models. In [2] several applications ranging from diffusion in porous media to interactions and reflections of shock waves in detonation problems are presented together with the analysis of the importance and the potential impact of errors.

A rigorous methodology to study failure analysis is introduced in [6] for a simple problem of imploding and exploring ring structure. The objective is to demonstrate that the system performance under a worst-case scenario remains above a given threshold. This QMU framework is used to explore different situations in which the computational model is assumed to be either exact or imperfect and various scenarios for uncertainty in the performance measures are considered. In particular, the authors explore how experimental data can be used to complement non-exact simulations. The QMU framework is based on formal bounds for the probability of exceeding stresses on the structure.

A more complex QMU analysis is reported in [5] where the thermal response of an engineering device under fire is studied. The complexity of the simulations and the need to rely on low fidelity computational models representing the system is discussed together with the importance of calibration and the difficulty in computing tails of probability distributions (failure probability).

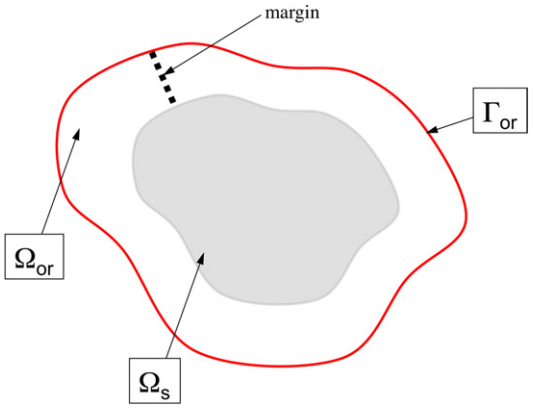

Fig. 1. Regions depicting the parameter space of an engineering system. Ω_{or} is the operating region, Γ_{or} represents the performance threshold and Ω_s the *safe* operation region.

The objective of this paper is to illustrate how a QMU analysis is formulated in a complex engineering problem where the interplay between fluid dynamics and thermal loads determine a performance threshold. In the following we will first briefly describe the operability limits of an air-breathing hypersonic vehicle and then introduce a relevant QMU framework. We will then describe a simple one-dimensional computational model of the propulsion system in order to explore the uncertainties associated with the system predictions. Finally, we will determine the safe operating region for a range of fuel flow rates and combustor configurations.

2. Operability limits of an air-breathing hypersonic vehicle

Air-breathing, hypersonic vehicles are highly integrated systems whose performance depends, to a very large extent, on the complex physics and interactions between all of their components. Such performance-critical systems cannot be credibly designed with today's state-of-the-art simulation capabilities not only because there are no available methods to predict the basic physical phenomena, but also because of uncertainties present in the actual flight environment, in the manufacturing of the various components, etc. As a result, the final design relies on extensive physical testing [7] and the introduction of conservative assumptions and safety constraints.

Of particular interest in this paper are the operability limits associated with the propulsion system of hypersonic vehicles flying at mid-range Mach numbers ($Ma \approx 8$). In these circumstances, the engine operates under supersonic conditions – scramjet mode – and a key *performance metric* is the amount of heat released in the combustion chamber, as it is directly connected to the generation of thrust.

Fig. 2 shows a schematic of the cross-section of a hypersonic vehicle. The presence of a supersonic flow stream over the entire vehicle logically introduces a *streamwise* splitting of the vehicle into several subsystems.

The forebody is dominated by the presence of the strong bow shock and the associated complex thermo-chemistry effects. The extreme heating occurring at the stagnation point determines the choice of materials and cooling strategies. As the flow decelerates towards the engine, boundary layers develop on the vehicle surface. Turbulence trips are designed to force transition to turbulence; in spite of the increased surface heating and friction, turbulent boundary layers entering the engine inlet lead to increased stability and mixing. The inlet/isolator system is

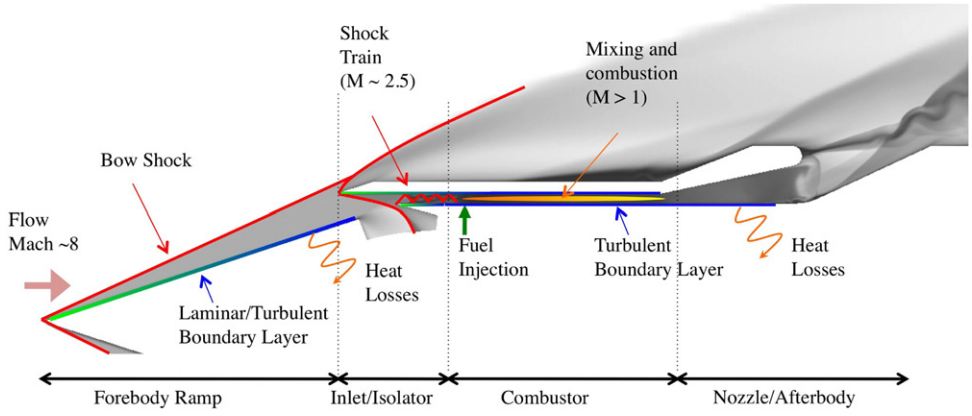

Fig. 2. Schematic representation of an air-breathing hypersonic vehicle.

designed to condition the flow towards pressure and temperature conditions that are most favorable to combustion. In addition, the shock train present in the isolator reduces the distortion of the incoming flow due to angle of attack and yaw variability. The combustor is the most critical component of the vehicle and, in particular, the injection system is carefully designed to mix the fuel and the incoming supersonic air stream and to produce auto-ignition of the mixture. Finally, the nozzle and afterbody further accelerate the flow stream producing thrust.

One of the main challenges in designing a scramjet engine is the extremely short residence time of the fuel within the combustor ($\sim$ ms); the ability to inject the fuel, mix it in the supersonic incoming air stream and ignite the resulting mixture is the critical design objective for the propulsion system. A minimum combustion efficiency (or heat release) is a performance threshold for the vehicle design. However, there is a well-identified limit to the heat release that can be *deposited* in a supersonic stream [8]. Excessive heating leads to *thermal choking*: a normal shock and a consequent subsonic flow region is established in the combustor. In addition to a reduction in the performance, this can lead to increased structural and thermal loads and eventually lead to *failure*. The normal shock can also propagate upstream in the combustion chamber, and eventually interact with the isolator, creating extensive regions of boundary layer separation; moreover, the shock motion can lead to engine *unstart* with the entire isolator shock train moving upstream. Under these conditions the vehicle performance is compromised and extreme actions have to be taken to *restart* the engine [7].

Unstart conditions can also be reached for different reasons, not directly connected to the combustion process. In particular, indications of unstart events connected to perturbations of the flow at the inlet [9] and to thermal deformations of the structure [10] have been observed in ground tests.

The objective of the present analysis is to characterize the thermal choking conditions and to quantify the margin associated with the unstart limit. In particular, it is clear from the above description that the engine performance (measured in terms of thrust) increases with the heat addition until it reaches the critical unstart limit, so it is desirable to operate the engine as close as possible to this *cliff*.

In the following we will introduce a highly simplified computational model to study scramjet performance and then we will describe the QMU framework for studying the confidence in the predictions.

2.1. Sources of uncertainty in the simulation of vehicle unstart

The unstart phenomenon is a complex thermal/fluid dynamic process that is critically sensitive to a variety of geometrical and physical parameters. It is useful to provide a characterization of the major sources of uncertainties in this process to guide the development of the QMU framework.

We can distinguish between various sources of uncertainty. The first group includes the imprecise characterization of the environment in which the vehicle is flying. Of these, we can assume that to leading order, the speed of flight, the angle of attack and the overall atmospheric conditions (mainly in terms of temperature fluctuations) will have the highest impact on the unstart predictions. Another large set of uncertain parameters is related to the material and *static* characterization of the vehicle. In this category we can include structural and material inhomogeneity, fuel mixture imperfections, surface roughness and, more generally, out-of-spec geometry. The final set of parameters are related to the thermal and fluid processes during flight: fuel injection rate, fuel temperature, combustion process, thermodynamic non-equilibrium at the leading edge, and the laminar-to-turbulent transition at the engine inlet.

Numerical predictions of hypersonic vehicle operations are based on computational tools that require models to simulate physical processes that cannot be treated from first principles. Therefore, a considerable level of uncertainty is also associated with the hypotheses and assumptions used in such models.

3. A reduced-order model for computing scramjet operability limits

Engineering analyses of scramjet propulsion systems have been carried out in the past [11] with the objective of designing access-to-space vehicles and high-speed commercial cruise airplanes. A comprehensive review of design methodologies is reported in Heiser et al. [12]: semi-analytical relations based on compressible gas-dynamics equations are derived and used to illustrate the various design choices.

The objective of the present analysis is not to design a new system but to analyze how computational tools in conjunction with experimental evidence can be used to identify safe operating conditions. The need to explore the thermal choking limit requires the construction of a phenomenological model that represents the unsteady nature of the flow in the scramjet and, eventually, unstart events. We seek the simplest approach that can represent an internal compressible flow with cross-sectional area change, heat release, unsteady effects and the occurrence of shock waves. The model we adopted is similar to that introduced by Bussing and Murman [13] and represents *only* the isolator, the combustion chamber and the nozzle (see Fig. 2).

The governing equations are

$$\mathbf{U}_t + \mathbf{F}_x = \alpha(\mathbf{P}-\mathbf{F}) + \mathbf{Q}/\mathbf{L}_c \tag{1}$$

with

$$\mathbf{U} = \begin{bmatrix} \rho \\ \rho u \\ \rho e \end{bmatrix}, \quad \mathbf{F} = \begin{bmatrix} \rho u \\ \rho u^2 + p \\ (\rho e + p)u \end{bmatrix}, \quad \mathbf{P} = \begin{bmatrix} 0 \\ p \\ 0 \end{bmatrix}, \quad \mathbf{Q} = \begin{bmatrix} 0 \\ 0 \\ Q_{comb} \end{bmatrix} \tag{2}$$

where

$$Q_{comb} = f_{st} H_f \dot{m}_f g(x/L_c) = \phi f_{st} H_f \dot{m}_o g(x/L_c) \tag{3}$$

ρ, u, e, p are the local density, velocity, total energy and pressure, respectively. $\mathbf{F}_x$ is the convective flux, whereas $\alpha(\mathbf{P}-\mathbf{F})$ on the right hand side represents the effect of the cross-sectional area change, $A(x)$, with $\alpha = (1/A)(dA/dx)$; L_c is the length of the combustor. Finally $\mathbf{Q}$ represents the heat addition with $\dot{m}_f$ and $\dot{m}_o$ being the mass flow rate of the injected fuel and the incoming air, respectively. f_{st} is the stoichiometric fuel/air ratio and H_f the fuel heating value. In the following analysis we will consider hydrogen as the fuel and, therefore, $f_{st}=0.029$ and $H_f = 1.2 \times 10^8$ J/kg$_{(H_2)}$. The equivalence ratio ϕ controls the amount of fuel injected.

The function $g(x/L_c)$ in Eq. (3) represents the distribution of heat release within the combustion chamber which is controlled by the precise fuel injector geometry, the turbulent mixing, and the kinetics of the auto-ignition and combustion process. In the present one-dimensional model, no attempt can be made to represent any of these phenomena realistically and, therefore, we assume a simple form of the heat release similar to [8]:

$$g(x/L_c) = \left(C_1 \frac{x}{L_c} \right)^{1/C_2} \tag{4}$$

where C_1 and C_2 are constants to be determined from experimental data.

The model is obviously a *very crude* approximation of the complex fluid flow environment within a scramjet. It is worth

mentioning the major assumptions that have been made (in addition to the one-dimensionality constraint): (i) absence of viscous effects, (ii) adiabatic walls, (iii) no mass addition due to the fuel injection and (iv) simplified heat release distribution due to the combustion process. It is possible to eliminate some of these assumptions; for example, the original formulation in [13] includes the effects of the viscous boundary layers on the walls by considering an effective cross-section area; it is beyond the scope of the present analysis to formulate a more comprehensive reduced-order model.

The equations are solved using a second-order finite volume discretization and an implicit time-integration scheme. Convective fluxes are evaluated using the approximate Riemann solver of Roe [14]. Boundary conditions are specified as fully supersonic at the isolator inlet with specified Mach number, Ma_i, total pressure, p_{t_i}, and total temperature T_{t_i}. The outflow conditions at the exit (nozzle) are specified as either supersonic or subsonic if thermal choking occurs.

In the following, we describe the formal process we followed to verify and validate the present reduced-order model.

3.1. Scramjet geometry and design conditions

Propulsion systems for hypersonic air-breathing vehicles are extremely simple systems compared to conventional jet engines; they have no moving parts, simple geometry and a very limited number of parts. In particular, the configuration is typically a straight or diverging duct (or pipe) with an end nozzle that produces most of the thrust. The fuel injection system is rather elaborate to improve mixing; the combustor is also a divergent duct to enhance stability and prevent unstart (we will exploit this in the following analysis of the operating margins).

The computational model described above creates severe limitations in our ability to represent the complex physical mechanisms in a scramjet propulsion system but it allows us to capture the overall geometrical configuration; specifically, we consider the geometry reported in [8]: a constant cross-section isolator of length 0.5 m is followed by a short combustor ($L_c = 0.1$ m) and a nozzle. Both the combustor and the nozzle are simple diverging ducts with angles of $\alpha_{comb} = 7.5^\circ$ and $\alpha_{nozzle} = 15^\circ$, respectively.

We will further assume that the engine inflow conditions correspond to $Ma_i = 2$ at the isolator entrance.

3.2. Unstart scenarios

In spite of the simplicity of the present model, we can represent realistic thermal choking scenarios; in particular we can investigate a staged increase of the fuel flow rate within the engine. The fuel addition leads to an increased thrust and the vehicle operates within the designed conditions until thermal choking occurs and a shock is formed within the combustor and propagates upstream.

All the simulations presented are carried out using the same sequence of events. Initially ($t \in [0 : 0.5$ ms]) a supersonic flow is established in the engine. Afterward, the fuel is injected in the combustor with a constant flow rate for a short time interval ($t \in [0 : 1.5$ ms]). Afterward ($t \geq 1.5$ ms) no fuel is injected. As an example, two different values of the fuel mass flow rate are considered in the calculations reported in Fig. 3. At the low fuel flow rate the flow remains supersonic throughout the scramjet; in the high fuel flow rate case, thermal choking occurs and a shock wave moves upstream into the isolator and eventually the engine is fully unstarted.

Interestingly the present model is also able to reproduce intermediate conditions as illustrated in Fig. 4. For a range of fuel flow rates, thermal choking occurs (detected by the presence of subsonic flow) and a shock is formed at the entrance of the combustor; nevertheless stable *burning* conditions are achieved; a slight increase in the fuel injection results in the shock moving with a slow velocity upstream. Once the fuel injection is terminated ($t = 1.5$ ms), supersonic conditions are again established (see Fig. 4) in both cases without unstart.

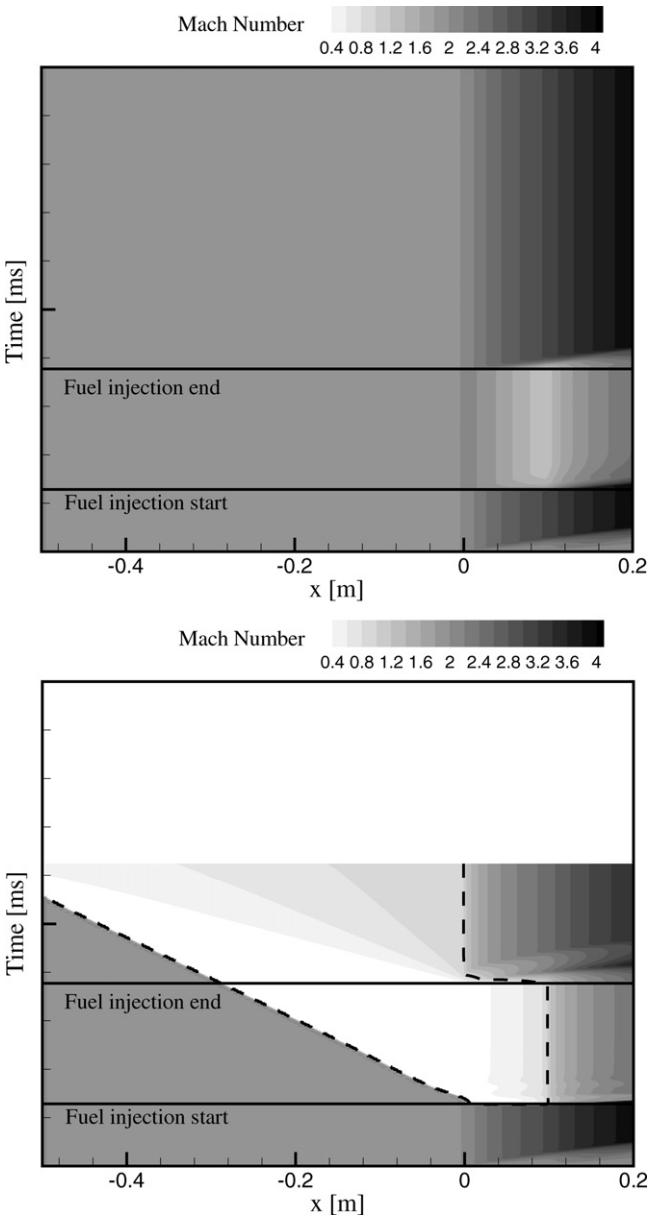

Fig. 3. Time/space plot of the Mach number within the simplified scramjet geometry. Fuel is injected with a constant flow rate between $t \in [0.5$ ms: 1.5 ms]. Low (top) and high (bottom) fuel flow rate are considered, leading to a stable operation of the engine and to unstart, respectively. The dashed black line is the sonic line which indicates if thermal choking occurred.

3.3. Quantity of interest

The fundamental feature of the unstart process is the formation of a normal shock wave traveling upstream in the isolator and eventually reaching the engine inlet. It is natural to consider the location and motion of the shock as the primary quantity of interest. Discontinuities create inherent difficulties for numerical algorithms and in the present approach we introduce artificial

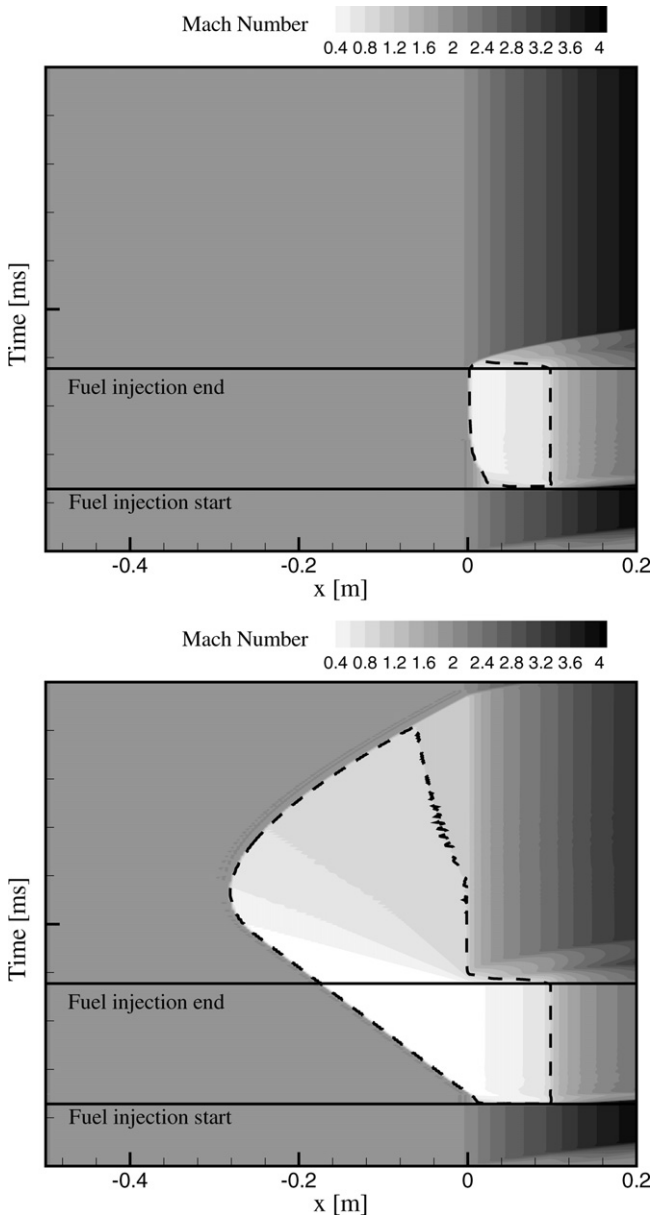

Fig. 4. Time/space plot of the Mach number within the simplified scramjet geometry. Fuel is injected with a constant flow rate between $t \in [0.5\text{ ms}: 1.5\text{ ms}]$. With the given fuel flow rate a shock initially moves upstream in the isolator, but supersonic conditions are recovered once the injection is terminated. The dashed black line is the sonic line which indicates if thermal choking occurred.

dissipation in the form of a low-order discretization in the vicinity of shocks. The addition of dissipation smears the discontinuity over several grid cells creating the additional challenge of precisely defining its position. In this work, we follow [15] by introducing a specific algorithm to reconstruct the shock location independently of the computational grid used: the density field in the vicinity of the shock is *reconstructed* using a hyperbolic tangent fit. At any given time, we assume a representation of the density profile in the form:

$$\rho(x) = \frac{\rho_L + \rho_R}{2} + \left[1 - \tanh\left(\frac{x_s - x}{2w}\right)\right] \tag{5}$$

where the parameters ρ_L, ρ_R, x_s and w are obtained using a least square minimization procedure starting from the computed density.

Table 1
Convergence rate for the shock tube problem. The L_2 norm of the error in density is defined in $x \in [3:4]$ and $t=2$ and p is defined using three successively refined grids [16]. x_s is the shock location computed using the hyperbolic tangent fitting, to be compared to the exact location $x_s=3.5043116$.

Cells	Δx	Δt	$L_2 \times 10^3$	p	x_s
100	0.1000	0.00200	0.68020	–	3.52890
200	0.0500	0.00100	0.34652	–	3.51720
400	0.0250	0.00050	0.18042	1.00640	3.51090
800	0.0125	0.00025	0.09992	1.04499	3.50760

3.4. Verification

The computational algorithm used to solve Eq. (1) has been applied to the classic time-dependent shock tube problem. Two chambers (left, L and right R) are filled with stagnating gas and separated by a diaphragm, that at time $t=0$ is fractured. The density ratio considered is $\rho_L/\rho_R = 8$ and the pressure ratio $p_L/p_R = 10$.

A quantitative comparison between the exact solution and the solutions obtained using two different grids (with 100 and 500 cells) is given in Table 1 where the L_2 norm of the error in density in the region around the shock wave ($x \in [3:4]$ and $t=2$) is reported. First order convergence in the vicinity of the discontinuity is expected given the numerical discretization employed.

The shock position computed using the hyperbolic fit is also reported in Table 1, showing that the increased grid resolution corresponds to better prediction of the shock location.

3.5. Calibration

The reduced model we introduced earlier is an extreme simplification of the complex injection, mixing and combustion processes occurring in a scramjet; the precise distribution of heat release has a strong impact on the characteristics of unstart and therefore, it is important to calibrate the model using relevant experimental data. The experimental study of [17] is used as a reference. The geometry is a simple, constant cross-section duct; the measurements were carried out for different equivalence ratios and inlet Mach numbers. The present model is calibrated using one set of data (corresponding to $Ma_i=2.5$ and $\phi = 0.4$) and then validated using two different operating conditions in the following section.

The objective of the present model is to reproduce the relation between the heat release in the chamber and the occurrence of a normal shock propagating upstream in the engine isolator. When comparing to measured data, the initial computed location of the shock always corresponds to experimental observations (the initial distance from the actual injector); this allows us to assess the ability of the model to reproduce the shock propagation speed which ultimately determines whether unstart will occur.

The shock locations measured in [17] are used to determine the two constants (C_1 and C_2) present in the heat release model. In Fig. 5 the results obtained using the calibrated model are compared to the reference data used; note that the experimental uncertainty is mainly associated with the determination of the shock location extracted from Schlieren images. The values of the constants in Eq. (4 are $C_1=4.21$ and $C_2=2.15$; these correspond to the best fit of the experimental shock location. Note that the values used in [8] were $C_1=3$ and $C_2=1$. Computations are also repeated assuming $\pm 5\%$ variation in the two constants to identify the variability associated with the present imprecise calibration; the results are reported as intervals in Fig. 5.

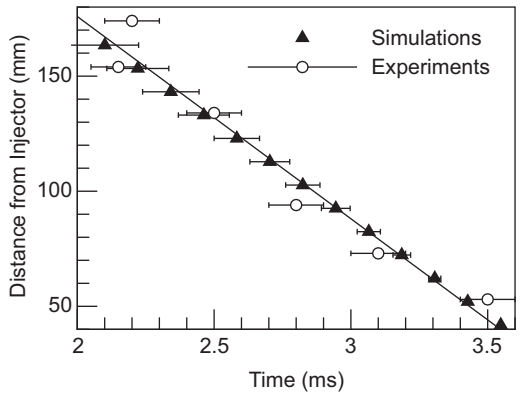

Fig. 5. Calibration results: computations of the shock speed for inlet Mach number of 2.5 and $\phi = 0.4$ (see [17]). The experimental data are used for calibrating the constants in the combustion model (Eq. (4)). The uncertainty bars in the simulations correspond to $\pm 5\%$ change in the model calibration constants.

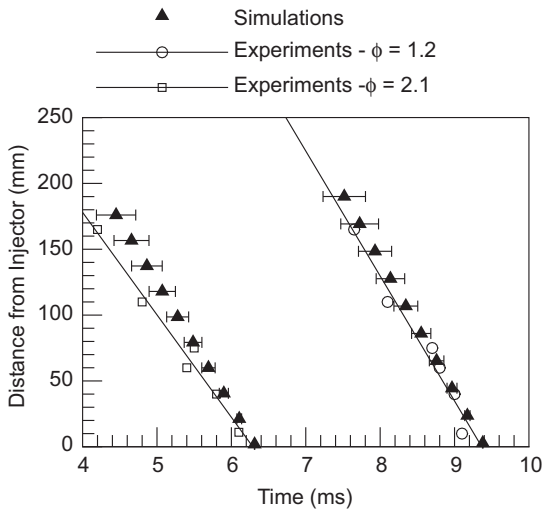

Fig. 6. Validation results: computations of the shock speed for inlet Mach number of 3.8 and $\phi = 1.2$ and $\phi = 1.7$ (see [17]) using the previously calibrated model. The uncertainty bars in the simulations correspond to $\pm 5\%$ change in the model calibration constants.

3.6. Validation

The calibrated model is used here to assess its capability to reproduce shock propagation speeds at various equivalence ratios. In particular, we again consider the experimental data set of [17] but we focus on higher inflow Mach numbers than those corresponding to the calibration test. As before, the accreditation is limited to the evaluation of the computed shock speed. The results for two values of the equivalence ratio are reported in Fig. 6 for an inflow Mach number of 3.5; the computations are also repeated changing the constant in the heat release model by 5%.

The computational results show that the present one-dimensional model represents the thermal choking and the subsequent normal shock formation and motion in a reasonable fashion, at least for moderately rich mixtures ($\phi \leq 2.0$). Results for higher fuel inflow rates could not be obtained because of numerical difficulties: the extreme heat release leads to choking immediately after the start of the fuel injection phase. A very strong shock is formed and this leads to spurious density oscillations. We conjecture that the simple heat release distribution assumed in the chamber (Eq. (4)) is not credible in the case of high fuel injection rate, because the effectiveness of the air/fuel mixing will likely determine an upper bound on the effective heat release.

4. QMU: quantification of margins and uncertainties

The first step in developing the QMU framework is to define one or more *figures of merit* (metric) to characterize successful operation of the scramjet engine. It is important that the chosen metrics be sensitive to all the important aspects of the prediction tools (and the experiments) used in the evaluation. In the present scenario the engine-generated thrust is the key characteristic of the propulsion system, and it is an obvious choice. Additional quantities could also be selected, such as the structural loads in the combustor, but for sake of simplicity only one metric is considered here.

In Fig. 7 a hypothetical thrust signature is reported; as the fuel flow rate is increased (or equivalently according to our model as the equivalence ratio ϕ is increased), combustion takes place in the engine. When a sufficient amount of heat is released in the mean supersonic stream, the pressure increases on the nozzle walls and leads to net thrust. As the fuel rate is further increased the amount of thrust can be adjusted. In Fig. 7 a lower bound corresponding to no net thrust is reported together with an upper bound associated with thermal choking that eventually leads to engine unstart. These two bounds characterize the *performance gate*, or the operating region in Fig. 1.

The confidence ratio, *CR*, must now be evaluated with respect to this critical gate, and indicates whether the system is operating safely within the performance gate; therefore we need to characterize both the margin and the uncertainties.

4.1. Margins

The margin is loosely defined as the desired distance between the performance threshold and the designed operation of the vehicle. As mentioned earlier, from a design perspective the highest thrust is achieved when operating as close as possible to the thermal choking limit.

Detailed experimental investigations have been carried out to identify the conditions that determine choking in the combustor; a notable example is the work of Owens et al. [18] who construct an empirical expression for the critical pressure in the combustor in the form:

$$p_{cr} = f(Ma_i, \dot{m}_f, A_i/A_e, \gamma) \tag{6}$$

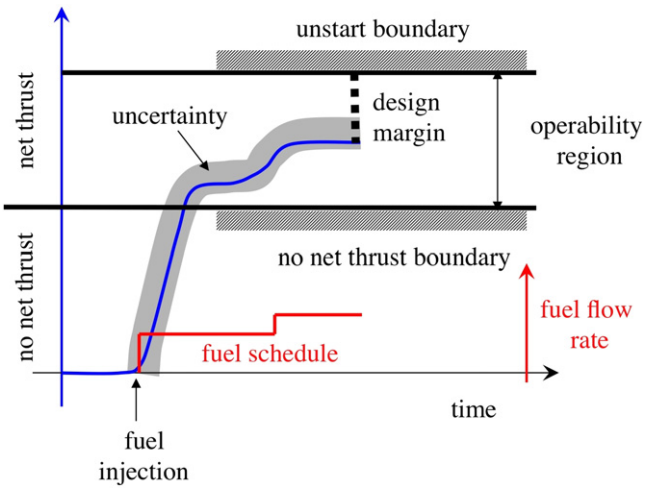

Fig. 7. Performance gate for the scramjet system.

where Ma_i is the entrance Mach number, $\dot{m}_f$ is the fuel flow rate, A_i and A_e are the entrance and exit cross-sectional area of the combustor (assumed to be simply a diverging duct) and γ is the ratio of the specific heats.

A more recent study [8] approached the problem from a theoretical perspective, using only thermodynamic laws and quasi-1D assumptions. As a final result they expressed the critical thrust (corresponding to thermal choking) in a form similar to Eq. (6).

As mentioned earlier, our goal is to illustrate the development and application of a QMU framework and, given the extreme simplification of the computational model, it is reasonable to consider a rather elementary measure of the thermal choking limit. We follow the experimental analysis in [19] and consider an upper bound on the ratio of the pressure in the combustor over the inlet pressure as the indicator for unstart; in this framework, Le [19] proposes a quadratic dependency of the bound with respect to the equivalence ratio; we will consider the same model.

The complex nature of the supersonic mixing and the auto-ignition process is not well understood and this leads to uncertainties in the determination of the upper bound on the amount of fuel that can be safely injected before unstart occurs. In particular, an increase in fuel flow rate can lead to an initial large heat release that triggers the inception of a normal shock and the formation of a subsonic region in the combustor. The initial upstream motion of this shock can lead to boundary layer separation; the resulting highly turbulent flow will be dominated by large vortical structures that can potentially lead to a reduction of mixing and local quenching, e.g. combustion will occur only in pockets within the combustor. The resulting reduction in the overall heat release could effectively stop the upward motion of the shock and lead to *recovery* and establishment of supersonic combustion conditions. In other words, the unsteady response of the engine to an increase of the fuel flow rate is critically controlled by the presence of large scale structures and the system might continue to operate normally even if temporarily above the static limit of heat release. The upper margin of Fig. 7 is therefore itself uncertain as it is controlled by time-dependent events that are quite stochastic in nature. In the present context, given the limited information available, it is appropriate to assume that the gate is characterized by an interval [20], as opposed to a probability distribution function [21]. Given the limited experimental evidence (for example [19, Fig. 6]) we *estimate* the uncertainty conservatively as $\pm 8\%$ of the pressure ratio. It is worth noting that the experiments in [19] only considered a combustor geometry characterized by a diffuser angle $\alpha_{comb} = 2.5^{\circ}$; we will assume that the diffuser angle in the combustor affects this bound in a linear fashion. In summary the upper bound estimate is expressed as

$$\frac{p_{cr}}{p_i} = (a\phi^2 + b\phi + c)(\alpha_{comb} - 1.5) \pm 8\% \tag{7}$$

where $a = 18.6$, $b = 14.8$ and $c = 1.40$.

The lower bound on the operating conditions is related to the ability to generate thrust, overcoming the aerodynamic resistance. In the application presented we will just assume a low value of p_{cr}/p_i as being the *no net-thrust* limit.

4.2. Uncertainties

Uncertainties are always abundant in complex engineering systems; the scramjet is no exception. Even in the simplest schematic representation of the engine, several sources of uncertainty must be accounted for as they can dominate the overall performance. In the present context, we will focus on *aleatory* uncertainties, associated with imprecise characterization of the various parameters affecting the engine operation, and epistemic uncertainty related to the calibration step presented earlier. In particular, we consider variability in flight conditions (inflow Mach number and total temperature), the thermodynamic state of the incoming air (changes in γ occurring because of potential thermal non-equilibrium effects at the bow shock), and the injected fuel mass flow rate. The *assumed* uncertainty is reported in Table 2.

Table 2
Uncertain quantities considered in the present study with the associated mean and *assumed* variability. Ma_i, T_{t_i} and γ characterize the inflow conditions, whereas C_1 and C_2 the uncertainty in the heat release model (Eq. (4)).

Quantity	Type	Mean	Bounds (%)
Ma_i	Aleatory	2.5	± 3
T_{t_i}	Aleatory	300	± 4
γ	Aleatory	1.4	± 5
C_1	Epistemic	4.21	± 5
C_2	Epistemic	2.15	± 5

The present computational model, on the other hand, is a very rudimentary representation of the rich thermal/fluid scenario within the engine. We are neglecting viscous effects, although it is well known that the interaction of shocks with boundary layers plays a crucial role in controlling the unstart progression. In addition, the entire engine is assumed to operate in adiabatic conditions and with fixed geometry, whereas in reality the thermal coupling between the flow and the structures is very important. We plan to address these and other sources of modeling uncertainties (*epistemic* uncertainty) in the future.

4.3. Confidence

Evaluation of the confidence ratio *CR* requires the calculations of measures of both margins and uncertainties. In a deterministic setting, the margin is simply the *distance* between the performance threshold and the design condition; given the variability in the performance estimate and the uncertainty in the unstart boundary, we must distinguish between the *expected margin* related to the best estimate of the bound and the operating condition and the *effective margin* which accounts for the presence of uncertainty; only the latter is of practical importance. The appropriate definition of the margin depends on the specific representation of the uncertain quantities.

Sharp et al. [20] introduced the concept of full and interval QMU to characterize the confidence in the two extreme cases when either probabilistic descriptions or only estimated ranges of the quantities of interest are available. Specifically, we define:

- *Full QMU*: The analysis is based on complete and precise probabilistic descriptions of all the quantity of interest. In this case, the *effective* margin relative to the upper boundary can be defined as (Fig. 8) by considering that for both the design conditions (subscript D) and performance threshold (subscript T) we can compute the mean (μ) and the standard deviation (σ) of the corresponding probability distributions. We define:

$$M = (\mu_T - n\sigma_T) - (\mu_D + n\sigma_D); \quad U = n\sqrt{\sigma_T^2 + \sigma_D^2}$$

  where n is the number of standard deviation values that correspond to a given confidence level. Note that with the above definitions, the metrics for both the margin M and the uncertainty U are described by a single value. Interestingly in this case the margin can be negative independent of the uncertainty in the bounds on the operability limit (inception of unstart).

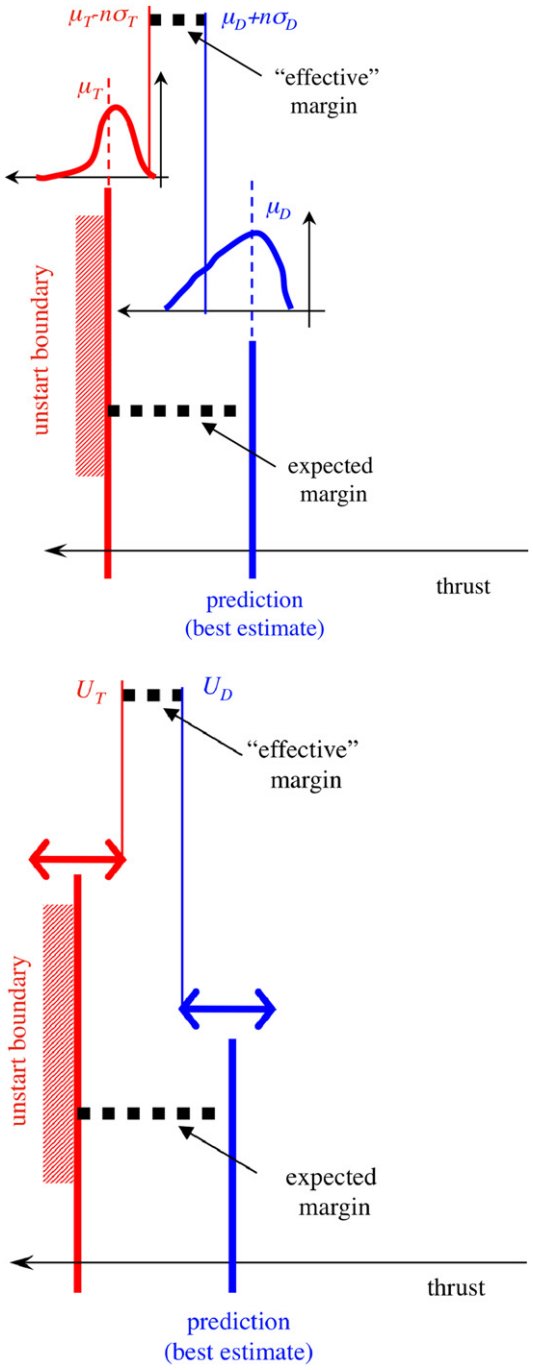

Fig. 8. Upper bound of the performance gate for the scramjet system (cfr. Fig. 7). The expected margin is defined as the distance between the performance threshold (subscript T) and the design conditions (subscript D). The effective margin accounts for the uncertainty in the evaluation of both quantities. Top: Full QMU—probability distribution for both the performance threshold and the design condition estimate are available. Bottom: Interval QMU—only intervals are available for both quantities.

- *Interval QMU*: the uncertainties are described using only ranges (intervals) without referring to probabilistic descriptions. This is a scenario compatible with lack-of-information and is considered in the analysis that follows. In this case, the uncertainty in the lower bound of the performance gate is simply given by U_T while the uncertainty in the upper bound of the operating region is given by U_D (see [20] for details of how to handle a combination of intervals and probability distributions). To evaluate the margin we define the expected performance threshold (μ_T) and design condition (μ_D) to be the mean of the respective intervals. In this case we define:

$$M = (\mu_T - U_T) - (\mu_D + U_D); \quad U = U_T + U_D$$

5. QMU analysis of thermal choking

Simulations are carried out corresponding to the nominal design conditions specified in Table 2. One of the problems in propagating the identified uncertainty in the computational code represented by Eq. (1) is the difficulty in representing both probabilistic (aleatory) and epistemic uncertainty. In the following examples we considered all the quantities to be represented as independent, uniform random variables and we used Monte Carlo sampling to characterize the output variability in terms of pressure distribution within the engine. In the analysis of the results we will consider the support of the output distributions as an interval with no associated probability distribution. It is possible to retain the probabilistic description of the aleatory uncertainties and reflect the corresponding distribution in the determination of the margins; one possible approach is to use a *nested sampling* strategy [22]. It is important to point out that such methodology would lead to an evaluation of *CR* that would be more complex that what afforded by either interval or full QMU.

Fig. 9 shows the pressure time-signal at two locations: within the nozzle and at the entrance of the combustor. The solution is highly sensitive to the input variability, especially at $x=0$.

More insight into the output uncertainty is presented in Fig. 10, where the coefficient of variation (COV) for the pressure is reported as a space/time plot. Note that in the present *interval analysis* the COV is defined as the midpoint of the interval over the range. Extremely high values of COV ($\approx 100\%$) occur close to the combustor entrance. These are representative of incipient unstart conditions, where under uncertainty a normal shock moves upstream.

5.1. Evaluating the confidence ratio

The evaluation of the confidence ratio *CR* requires the calculations of both margins and uncertainties. We performed Monte Carlo simulations to account for the uncertainties introduced before, and we used a fixed geometry and a number of different fuel injection conditions. The objective is to study the operating region of the scramjet, as the probability of engine unstart increases as the more fuel flow rate increases. In Fig. 11 the results of this analysis are reported in terms of the pressure within the combustor; two different behaviors emerged, corresponding to normal operation (supersonic flow throughout the system) and to the occurrence of a shock in the combustion chamber and, therefore, to engine unstart. This abrupt change of behavior is completely determined by the uncertainties present, since the nominal inputs of the model are selected according to safe operating conditions. From Fig. 11 we can readily evaluate the margin and the uncertainty in the quantity of interest for each value of the equivalence ratio. It is clear that the uncertainty in the *unstart bound* also grows considerably as the equivalence ratio is increased. It is important to note that the accuracy of the predictions during an unstart event is questionable, because the present model ignores viscous interactions that will dominate the dynamics of the upstream moving shock. For this reason in Fig. 11(bottom), we replaced the predicted unstart bound (reported in Fig. 11(top)) with the experimental correlation – and the reported uncertainty – introduced in [18]. This results is a

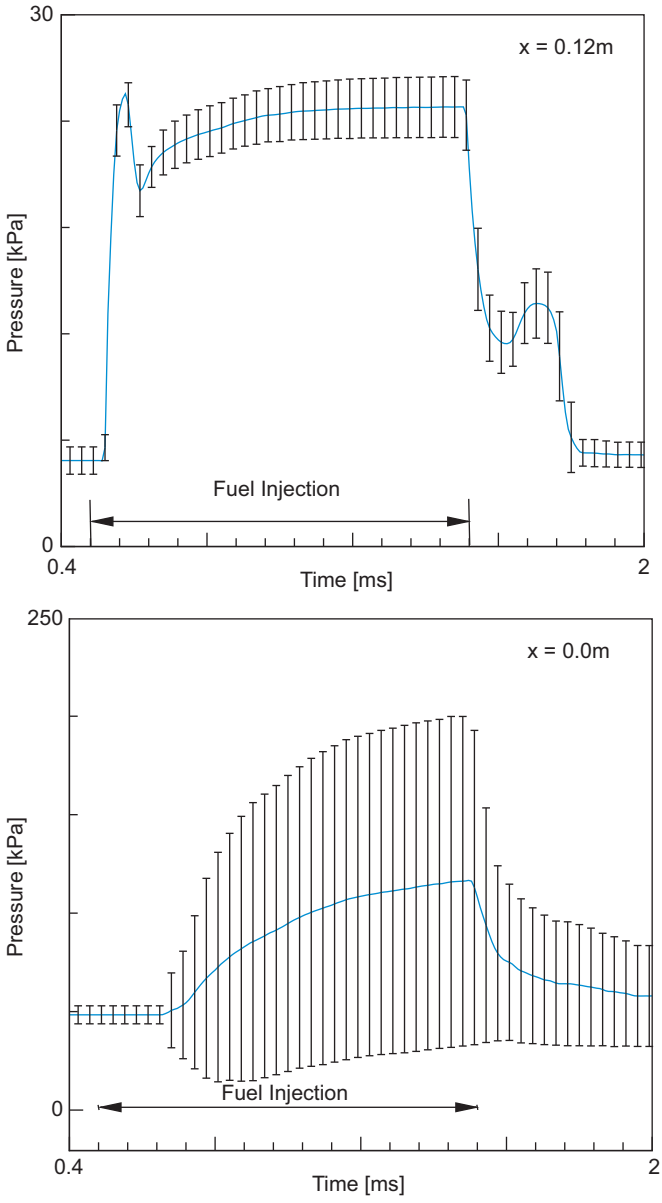

Fig. 9. Predictions of the pressure within the engine: towards the nozzle exit (top) and at the entrance to the combustor (bottom). Bars represent 95% confidence bounds obtained performing Monte Carlo simulations.

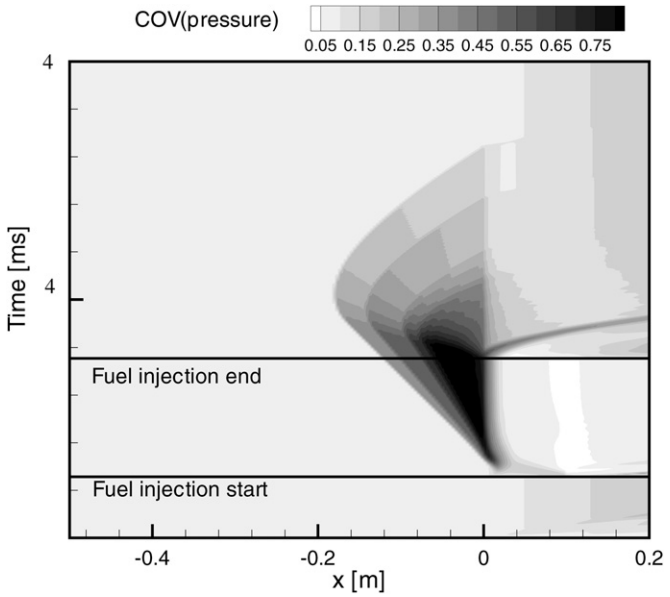

Fig. 10. Space/time plot of the coefficient of variation of the pressure within the scramjet engine.

somewhat smaller margin at low equivalence ratio, but a considerably smaller uncertainty at higher fuel flow rates.

5.2. QMU for system design

The primary objective of QMU is to evaluate the confidence (and reliability) of a system for a range of design conditions. In the present context, we are not targeting a particular scramjet, and it is therefore more useful to illustrate how a QMU framework can be used to evaluate the interplay between operability limits and design choices. The thermal choking limit is strictly a thermodynamic phenomenon: the deceleration of a supersonic stream in the presence of heat addition eventually leads to the formation of a normal shock. On the other hand, the unstart phenomena triggered by the thermal choking is determined by a pure fluid-dynamics process: the upstream motion of the normal shock within the isolator. From the example illustrated before (see for example Fig. 3(top)) it is clear that even in the presence of thermal choking the upstream propagation of the normal shock can be avoided by considering a diffuser-shaped combustor; in fact, in theory the larger the angle α_{comb} the more heat release can be accommodated in the combustor. From a fluid dynamics perspective the upstream shock propagation is inhibited by the adverse pressure gradient environment.

Our objective is to compute the QMU confidence ratio for a combination of equivalence ratios and combustor diffuser angles, so as to construct the *safe* operation region for a generic scramjet engine. We performed computations similar to those illustrated earlier where the fuel is injected for 1 ms ($\phi \neq 0 \in [0.0004: 0.0016]$ ms) at a constant equivalence ratio. We *define* unstart to occur when a shock is detected at a certain location in the isolator ($x = -0.4$ m) within a time window of 4 ms ($t \in [0: 0.004]$ ms). The computations are repeated for $\phi \in [0: 1.6]$ and $\alpha_{comb} \in [0: 12]$.

The results are presented in terms of a *confidence ratio map*, reported in Fig. 12. The points where $CR > 1$ correspond to safe operation conditions. It is worth noting that two *artificial* boundaries have been added to the plot in Fig. 12. The right boundary, namely the flow separation limit, is related to the eventual flow separation induced by large diffusion angles in the combustor. The present model is unable to capture this phenomenon, but it is expected that after a certain angle the interaction of the shock in the combustor and the boundary layers will create a large separation that eventually will lead to loss of thrust; we assumed for simplicity that this bound corresponds to a given diffuser angle. The second boundary (represented by the lower curve in Fig. 12) indicates the minimum value of the thrust that is required for acceptable vehicle performance. This bound can only be evaluated if additional information on the system configuration is given; here we assumed that the thrust is directly proportional to the injected fuel (ϕ) and that the diffuser angle in the combustor contributes to create thrust. In the present analysis we assumed that these two bounds are known as they are not directly related to the thermal choking phenomenon.

The *CR* factor is evaluated by performing Monte Carlo simulations at each point in the $\phi - \alpha_{comb}$ plane; in practical terms *only* 8×8 analyses (each one consisting of 1000 independent realizations aimed at characterizing the uncertainty described in Table 2) were carried out and the results interpolated to construct the curves in Fig. 12. The results show several interesting features,

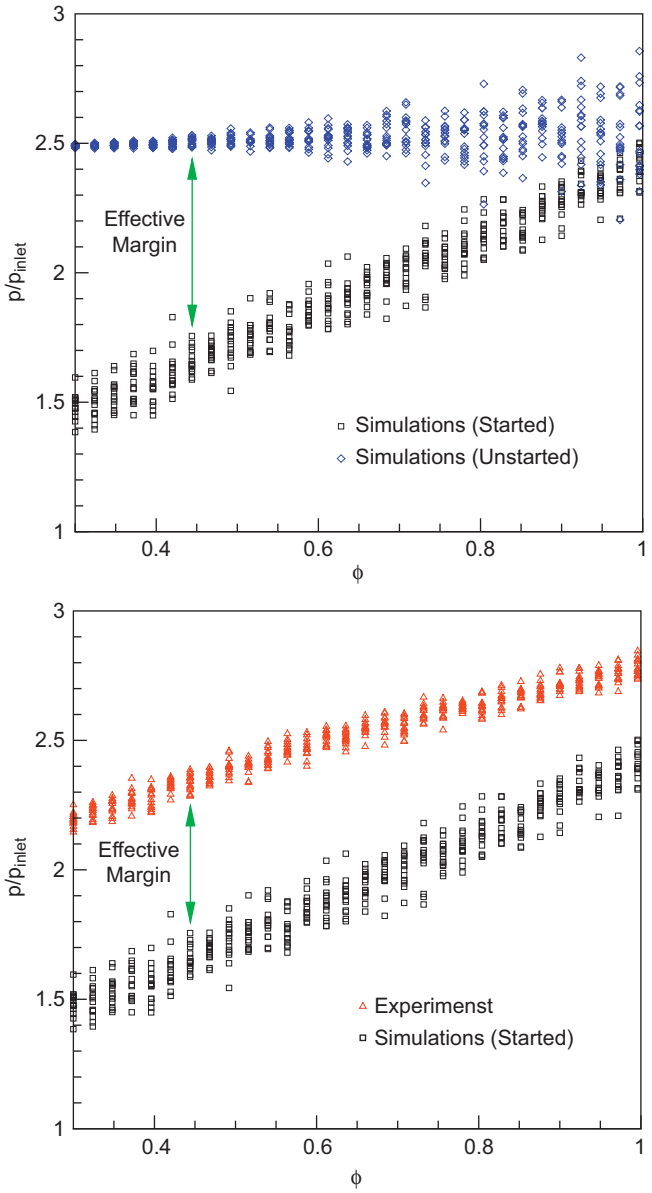

Fig. 11. Evaluation of unstart margin for a range of fuel equivalence ratios. The unstart boundary is evaluated using the current computational model (top) and an experimental correlation (bottom) [18].

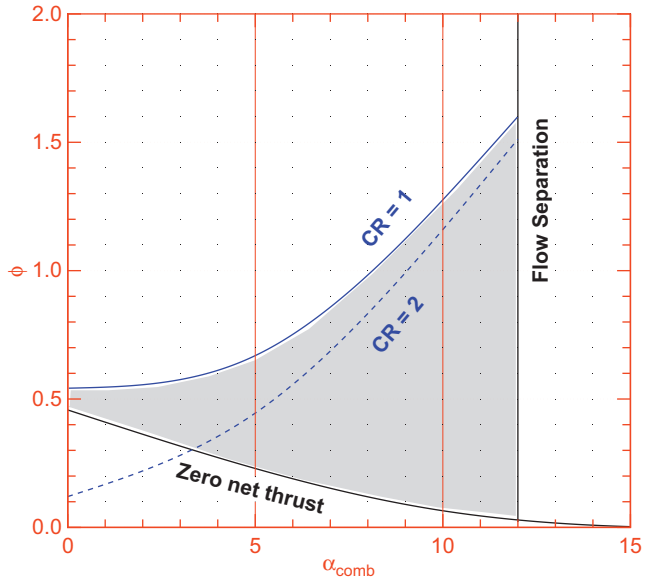

Fig. 12. Unstart boundaries due to thermal choking for two required confidence ratios as a function of the equivalence ratio and the diffuser angle in the combustor. The grey area corresponds to the *safe* operation region (Ω_s in Fig. 1). The minimum thrust and the flow separation bounds are assumed.

the two most important observations from a scramjet operation perspective are:

1. For a straight combustor geometry ($\alpha_{comb}=0$) the operating region is very narrow in terms of the injected fuel equivalence ratio. Increasing the demand on the *reliability* (demanding a larger confidence ratio) leads to an unfeasible design.
2. The safe operating region expands with α_{comb}: physically this is due to the increased ability to stabilize a normal shock in the combustor resulting from the diffuser angle in the combustor. For large diffuser angles an increased reliability demand does not shrink the operability range considerably.

Finally, it is useful to note that the presence of two other boundaries in Fig. 12 naturally leads to the need to define a more comprehensive model of the scramjet flow/thermal environment than the one employed in this study. The lower bound on the vehicle thrust can be defined according to typical design considerations [12]; on the other hand, the bound on the right – the flow separation limit – requires a considerably more sophisticated model involving the solution of two- or three-dimensional reacting flow equations. In addition the QMU analysis also requires the determination of a theoretical/experimental limit for the corresponding bound, which in the case of flow separation can be extremely challenging.

From a computational perspective, the construction of a map such as that shown in Fig. 12 is a formidable undertaking. 64,000 independent unsteady simulations were carried out; given the extreme simplicity of the present reduced-order model each computation is completed in less than 10 s and, therefore, all the simulations were completed in about a day on an 8-cores desktop. Each solution corresponds to a point in the $\phi-\alpha_{comb}$ plane and provides one evaluation of the (possible) presence of a shock traveling upstream towards the scramjet inlet.

In Fig. 12 an additional line corresponding to $CR=2$ is reported. This line indicates the operating conditions that lead to an increased performance margin, or equivalently that are less dominated by uncertainties. In the present context the CR represents a metric that is equivalent to an engineering safety margin and can be used as a *free* parameter to explore different configurations and design choices. An additional interpretation of the difference between the $CR=2$ and the $CR=1$ lines is the performance gain that can be obtained by reducing the uncertainty by 50%; the results in Fig. 12 show that for low combustor angles the increase in the amount of fuel allowed without unstarting the engine is considerable, whereas only a limited change is observed for large value of α_{comb}.

6. Conclusions

The QMU analysis presented here is the first step towards a comprehensive analysis of failure modes in a scramjet engine using computation. We define a simplified simulation framework capable of reproducing qualitatively thermal choking and the eventual engine unstart. This model was verified and then calibrated against experimental data corresponding to a simple straight duct configuration. A validation step was also carried out to assess the accuracy of the simulations. In a second phase, uncertainty in both the inlet

conditions and the calibration constants in the heat release model were evaluated to identify their impact on the unstart scenario. Finally the performance threshold corresponding to unstart triggered by thermal choking was identified and analyzed.

Future work will focus on the introduction of a more comprehensive computational model to represent the reactive flow in the scramjet. The inclusion of viscous effects is clearly of primary importance in the characterization of the unstart boundaries, together with a better representation of the mixing, combustion and heat release in the combustion chamber. In addition, we intend to pursue a more complete characterization of the margins, by introducing multiple gates that represent in more detail the sequence of physical processes that contribute to determine the performance thresholds. The extension of present QMU framework to include multiple gates is a very important and challenging endeavor.

Acknowledgments

This material is based upon work supported by the Department of Energy [National Nuclear Security Administration] under Award number NA28614.

The present manuscript also appears as a Los Alamos preprint LA-UR 09-01863.

References

[1] Sharp DH, Wood-Schultz MM. QMU and nuclear weapons certification. What's under the hood? Los Alamos Science 2003;28.
[2] Christie MA, Glimm J, Grove J, Higdon DM, Sharp DH, Wood-Schultz MM. Error analysis and simulations of complex phenomena. Los Alamos Science 2005;29.
[3] Eardley D (Study Leader). Quantification of margins and uncertainties (QMU). Technical Report JSR-04-330 (JASON); 2005.
[4] Pilch M, Trucano TG, Helton JC. Ideas underlying quantifications of margins and uncertainties (QMU): a white paper. SAND2006-5001; 2006.
[5] Romero VJ. Some issues and needs in quantification of margins and uncertainty (QMU) in complex coupled systems. AIAA Paper 2006-1989, AIAA; 2006.
[6] Lucas LJ, Owhadi H, Ortiz M. Rigorous verification validation uncertainty quantification and certification through concentration-of-measure inequalities. Comput Methods Appl Mech Eng 2008;197(51–52):4591–609.
[7] Huebner LD, Rock KE, Ruf EG, Witte DW, Andrews EH. Hyper-X flight engine ground testing for X-43 flight risk reduction. AIAA Paper 2001-1809, AIAA; 2001.
[8] Riggins D, Tackett R, Taylor T, Auslender A. Thermodynamic analysis of dual-mode scramjet engine operation and performance. AIAA Paper 2006-8059, AIAA; 2006.
[9] Sato T, Kaji S. Study of steady and unsteady unstart phenomena due to compound choking and/or fluctuations in combustor scramjet engines. AIAA Paper 1992-5102, AIAA; 1992.
[10] Buchmann OA. Thermal-structural design study of an airframe-integrated scramjet. NASA CR 3141. In a model scramjet engine. J Prop Power 1979;16(5):808–14.
[11] Curran ET. Scramjet engines: the first forty years. J Prop Power 2001;17(6).
[12] Heiser WH, Pratt DT, Daley DH, Mehta UB. Hypersonic air-breathing propulsion. Washington, DC: American Institute of Aeronautics and Astronautics; 1994.
[13] Bussing TRA, Murman EM. A one dimensional unsteady model of dual scramjet operation. AIAA Paper 83-0422, AIAA; 1983.
[14] Roe PL. Approximate Riemann solvers, parameter vectors, and difference schemes. J Comput Phys 1981;43:357–72.
[15] Yu Y. Errors in numerical solutions of shock physics problems. PhD thesis, SUNY at Stony Brook; December 2004.
[16] Roache PJ. Verification and validation in computational science and engineering. Albuquerque, NM: Hermosa Publishers; 1998.
[17] O'Byrne S, Doolan M, Olsen SR, Houwing AFP. Analysis of transient thermal choking processes in a model scramjet engine. J Prop Power 2000;16(5): 808–14.
[18] Owens MG, Mullagirl S, Segal C, Ortwerth PJ, Mathur AB. Thermal choking analyses in a supersonic combustor. J Prop Power 2001;17(3):611–6.
[19] Le DB. Scramjet isolator flow studies. PhD thesis, University of Virginia; 2002.
[20] Sharp DH, Wallstrom TC, Wood-Schultz MM. Physics package confidence: one vs. 1.0. LAUR-04-0496, Los Alamos; 2004.
[21] Pepin JE, Rutheford AC, Hemez FM. Defining a practical QMU metric. AIAA Paper 2008-1717, AIAA; 2008.
[22] Jakeman J, Eldred M, Xiu D. Numerical approach for quantification of epistemic uncertainty. J Comput Phys 2010;229:4648–63.